Technologies for the Next Generation of Spaceborne Precipitation Radars

Greg Sadowy, Andy Berkun, Steve Durden, John Huang, Eastwood Im, Bernardo Lopez, Michael Lou
Jet Propulsion Laboratory, California Institute of Technology
4800 Oak Grove Drive, M/S 300-241
Pasadena, CA 91109
818-354-1467
sadowy@jpl.nasa.gov

Yahya Rahmat-Samii, Fan-Yun Liu
University of California, Los Angeles
Los Angeles, CA 90095-1594
rahmat@ee.ucla.edu

Sembiam Rengarajan
California State University, Northridge
Northridge, CA 91330
srengarajan@csun.edu

Abstract—The precipitation radar (PR) aboard the Tropical Rainfall Measuring Mission (TRMM) has demonstrated the feasibility of measuring rainfall from space. A concept for the next step, the Second Generation Precipitation Radar (PR-2), has been developed. The PR-2, which will yield improved capabilities and substantially reduced system mass compared to the TRMM PR. However, implementation of the PR-2 concept depends upon the development of several technologies including, membrane antennas with inflatable structure, Ka-band phased arrays, and real time digital pulse compression. Development is currently underway in these areas. This paper surveys the technologies for the PR-2 and describes developments in each aforementioned area.

TABLE OF CONTENTS

1. INTRODUCTION

The Precipitation Radar (PR) aboard the Tropical Rainfall Measuring Mission (TRMM) satellite has successfully demonstrated the feasibility of measuring rainfall using spaceborne radar [1]. However, it is desirable for future rainfall measuring missions, such as NASA's planned Global Precipitation Mission (GPM) to both enhance the performance of the precipitation radar and reduce its mass. To these ends, a system concept using a dual-frequency radar with a deployable 5.3-meter electronically-scanned membrane antenna and real-time digital signal processing has been developed. This new system, the Second Generation Precipitation Radar (PR-2), will offer greatly enhanced capability with a fraction of the mass of the current TRMM PR [2].

Implementation of this new concept requires the development of new technologies in several areas, including membrane antennas, active phased arrays and real-time digital signal processing. A key element of this system is a 5.3-meter parabolic-cylindrical membrane reflector that employs an inflatable, rigidizable structure. Building on current developments of flat membrane antennas, a preliminary design of a singly curved membrane reflector has been created and analyzed. Effects of thermal distortion, mechanical resonances, random error, and manufacturing tolerances were modeled and simulations were used to demonstrate the feasibility of this approach at both Ku (13.4 GHz) and Ka-band (35.6 GHz).

An innovative adaptive scanning algorithm is used to maximize the fraction of sampling time devoted to measuring rain-filled pixels, thereby effectively increasing the swath width. The requirement for highly agile cross-track scanning using the parabolic cylindrical reflector dictates the use of a phased-array line feed. This line feed consists of two active dual-polarized phased arrays. Currently, a subarray prototype of the Ka-band active array is being developed. This array incorporates miniaturized, active T/R modules, each capable of delivering 1W of output power and receiving on two orthogonal linear polarizations. The module incorporates up and down-conversion, phase shifters, low-noise amplifiers, transmit drivers and power amplifiers. Dual polarization operation is

achieved by using a miniature orthomode transducer (OMT), allowing the entire module to be less than 5 mm thick.

Another key innovation required to implement the PR-2 system is real-time digital pulse compression. Aircraft experiments with the Airborne Rain Mapping Radar (ARMAR) have demonstrated digital pulse compression with nearly 60 dB of range sidelobe suppression [3]. This high level of range sidelobe suppression is required for down looking rain radars to prevent strong surface echoes from obscuring weak echoes from light rain near the surface. In order to avoid the tremendous burden of storing and downlinking raw radar data, as was previously done when digital pulse compression was used, the PR-2 will use an FPGA-based signal processor to implement digital pulse compression and data averaging in real time. Sixty-four pulse compressed returns are averaged before downlinking, yielding a substantial reduction in downlink data rate. An airborne testbed for this real time processing technology is currently being developed. A flight breadboard is also being developed in order to demonstrate a robust FPGA-based processing architecture that is tolerant of single event upsets and will operate with high reliability in the low Earth orbit environment.

2. ANTENNA SELECTION

A detailed study of tradeoffs at the system level was used to determine the requirements for the PR-2 antenna. The requirements that influence the design most strongly are the aperture size required to achieve the desired resolution, the sidelobe level required to avoid contamination of rain echoes by the surface returns and the scan agility which is required to implement the adaptive scanning algorithm. With these primary objectives in mind, three antenna configurations were evaluated.

Slotted Waveguide Array

The planar waveguide array has the advantage of being a simple planar structure and relatively low RF insertion loss. A number of configurations involving waveguide-fed planar slot arrays were studied. We determined that the shared aperture configuration is not feasible because of the low sidelobe requirement. If shared Ka- and Ku-band waveguides are used, unacceptable grating lobes will be generated when the array is scanned away from broadside. Therefore, two separate apertures are required. Because of the large aperture required at Ku-band, a deployable antenna is required. Designing folding mechanisms for the waveguides that do not compromise their electrical performance would be quite challenging. Additionally, the slotted waveguide approach would have relatively large mass compared to competing concepts.

Reflectarray

The second option studied was a flat array of passive radiating elements (reflectarray). This array is composed of a multilayer membrane covered with isolated microstrip patches. Each patch has two stubs attached (one for each polarization) that control the reflection phase of that element. By controlling the length of the stubs a planar wavefront can be constructed. In the central region of the reflector, three layers are used to accommodate dual-frequency shared-aperture patches. In the outer regions, only Ku-band patches are used.

The 5.3 m x 5.3 m membrane stack can be deployed using inflatable structures. Because the reflectarray is a flat, natural surface, it is easier to achieve the required surface tolerance than it would be for a curved surface. However, a multifrequency, multipolarization shared aperture reflect-array has yet to be demonstrated and would entail substantial additional complexity and risk. It would be particularly challenging to meet the stringent sidelobe requirements using this configuration.

Cylindrical Membrane Reflector

The concept selected for further study was a singly curved deployable membrane reflector. The membrane has parabolic curvature in the along-track direction and is flat in the cross-track direction. Cross-track gain is achieved by using two linear array feeds (one of Ku-band and one for Ka-band). This membrane can be deployed using inflatable structures, which are curved to form the required parabolic shape. This antenna configuration is shown in Fig. 1. Since the membrane reflector is simply a metalized surface, it is inherently broadband and therefore is able to accommodate both Ku-band and Ka-band frequencies. This eliminates the complexities of a multilayer, dual-frequency, dual-polarization patch scheme of the flat reflectarray.

3. REFLECTOR ELECTRICAL DESIGN

The key requirements for the membrane reflector are low sidelobe level and matched beams for both frequencies. Low sidelobe levels are required to prevent contamination of precipitation echoes with energy from surface echoes. When the antenna is scanned off nadir, the echo from the surface at nadir arrives at the same time as precipitation echoes from off-nadir beams. Since the specular return from the surface can be 60 dB stronger than the rain echoes, one-way sidelobe suppression of at least 30 dB is required.

The matched beams at Ku- and Ka-bands are required to implement dual-frequency rain-rate retrieval algorithms, which have been shown to improve retrieval accuracy over single frequency algorithms. To achieve matched beams, the reflector is underilluminated at Ka-band. By fully illuminating the reflector at Ka-band, higher sensitivity could be achieved, but the Ka-band radar sample volume
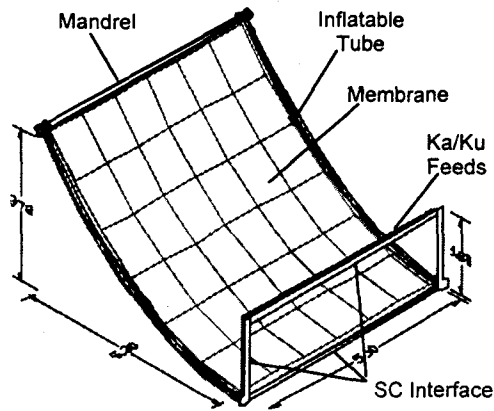
Fig.1. Membrane antenna configuration

Table 1. Ku-band beamwidth and directivity

F/D	Scan angle (deg.)	Directivity (dB)	Beamwidth (deg.)
0.35	0	56.2	0.14
0.35	37	50.4	0.25
0.60	0	56.8	0.14
0.60	37	47.3	0.32

Table 2. Ka-band beamwidth and directivity

F/D	Scan angle (deg.)	Directivity (dB)	Beamwidth (deg.)
0.35	0	55.7	0.15
0.35	37	55.0	0.20
0.60	0	56.3	0.16
0.60	37	48.5	0.32

would be substantially smaller than the Ku-band sample volume. Inhomogeneity of the precipitation would introduce unresolved biases into the dual-frequency rain rate retrievals. Underillumination of the reflector solves this problem while still providing adequate sensitivity at Ka-band.

Reflector Configuration

Several studies were conducted in order to evaluate design tradeoffs and to predict the performance of the reflector antenna. A key design parameter of the parabolic cylindrical reflector is the focal length. Longer focal lengths result in a flatter surface, which reduces unwanted cross-polarized components and is also easier to maintain mechanically. However, increased focal length increases spillover losses, differential path length losses and requires a larger and heavier structure to hold the feed array.

Two configurations, with an F/D of 0.35 and 0.60 were evaluated. Studies of the effects of aperture blockage by the feed array suggested that an offset-fed configuration was preferred. An idealized feed array was modeled using a cos^q radiation pattern. The reflector was illuminated using this idealized feed pattern and the reflector far-field patterns were computed using the physical optics approximation. The results of these computations for both Ku-band and Ka-band are shown in Tables 1 and 2 respectively. The performance at broadside is acceptable for both F/D at both frequencies. However, when the beam is scanned to the maximum angle (37°), the directivity and beamwidth degrade much more rapidly for F/D equal to 0.6. This is true for both frequency bands. This beam broadening and reduction in directive gain is due to increased spillover when the feed array is scanned. The effect is more pronounced at Ku-band because the reflector is underilluminated at Ka-band.

As expected, the cross-polarization characteristics of the 0.6 F/D configuration were somewhat superior but the crosspol performance of the 0.35 F/D configuration was deemed acceptable. Since the 0.35 F/D configuration provides narrower beamwidth at larger scan angles, and requires
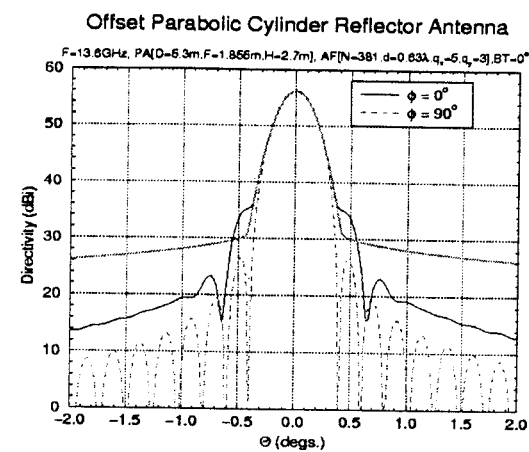
smaller feedhorns and feed support structure, F/D equal to 0.35 was chosen for further study.

Another configuration parameter is the tilt angle of the Ka-band feed. The Ku-band feed is pointed at the center of the reflector in order to minimize spillover. However, because the Ka-band feed under illuminates the reflector, there is a range of tilt angles that could be used without substantially increasing spillover. In offset-fed configurations, the crosspolarized component increases as the tilt angle increases.
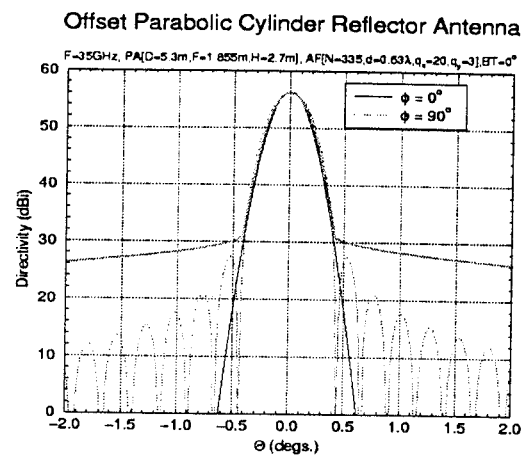
Far field patterns were calculated for Ka-band feed tilt angles of 72°, 60° and 45°. Zero degrees is the reference symmetry axis of the parabola. Examination of the radiation patterns revealed that while the copolarized directivity was relatively insensitive to tilt angle, the crosspolarized component was strongly affected. The 45° tilt angle exhibited 14 dB less crosspolarized component than the 72° tilt angle studied. Thus it is advantageous to use the smallest tilt angle possible without incurring unacceptable spillover losses.
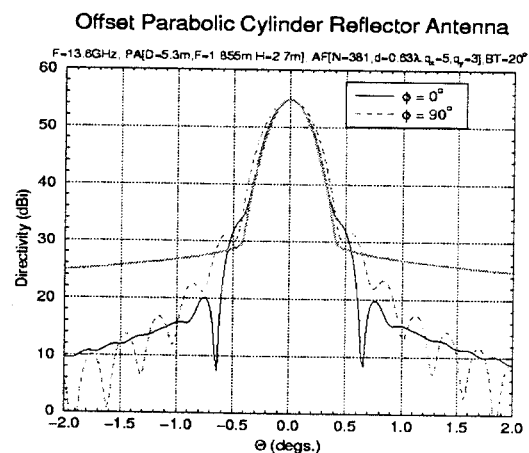
Reflector Performance

Once the reflector configuration was determined, a realistic model of the feed system was developed. The simple cos^q model used for the configuration tradeoff studies was computationally efficient but is not sufficiently realistic to accurately determine the performance of the overall antenna system. If q_x and q_y (q values in two orthogonal directions) are chosen to give the proper illumination of the reflector, accurate copolarized reflector patterns can be computed. However, if the ratio between q_x and q_y is large, the pattern will contain high cross-polarized components that would not occur in the pattern of a real feed element such as a pyramidal horn. Instead of computing patterns of real horn elements, which is computationally inefficient, each array element is modeled as an array of cos^q elements with the number of elements chosen such that the horn pattern is closely approximated and the ratio q_x/q_y is close to one. This
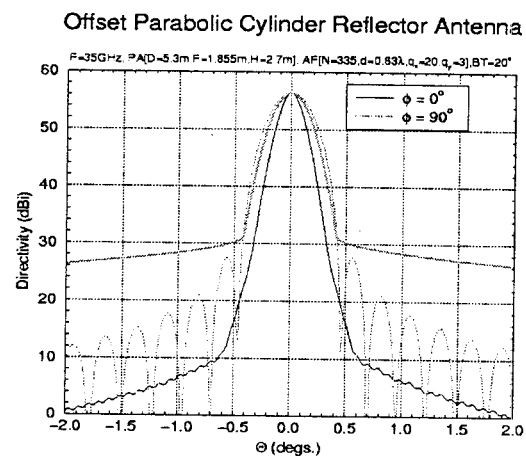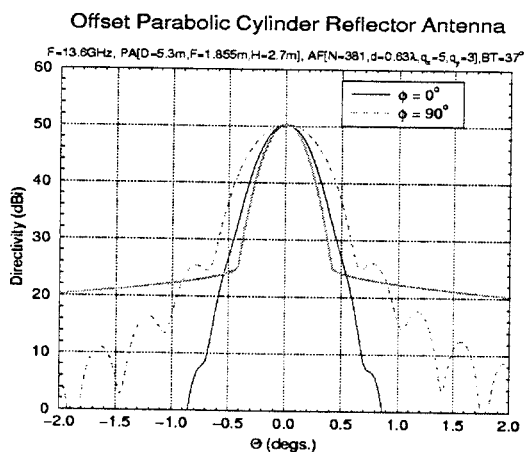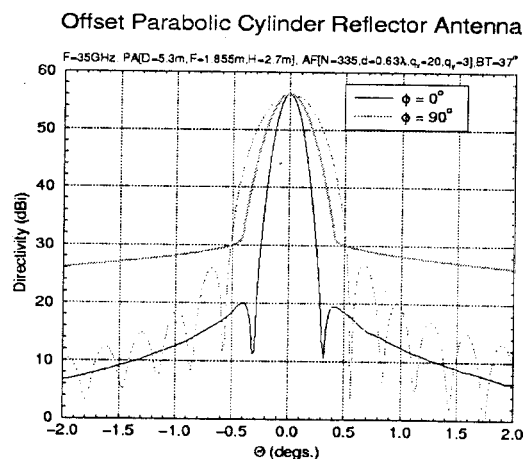
Offset Parabolic Cylinder Reflector Antenna

F=13.6GHz, PA[D=5.3m,F=1.855m,H=2.7m], AF[N=381,d=0.63λ,q_s=-5,q_y=-3],BT=0°

a)

Offset Parabolic Cylinder Reflector Antenna

F=13.6GHz, PA[D=5.3m,F=1.855m,H=2.7m], AF[N=381,d=0.63λ,q_s=-5,q_y=-3],BT=-20°

b)

Offset Parabolic Cylinder Reflector Antenna

F=13.6GHz, PA[D=5.3m,F=1.855m,H=2.7m], AF[N=381,d=0.63λ,q_s=-5,q_y=-3],BT=37°

c)

Offset Parabolic Cylinder Reflector Antenna

F=35GHz, PA[D=5.3m,F=1.855m,H=2.7m], AF[N=335,d=0.63λ,q_s=-20,q_y=-3],BT=0°

d)

Offset Parabolic Cylinder Reflector Antenna

F=35GHz, PA[D=5.3m,F=1.855m,H=2.7m], AF[N=335,d=0.63λ,q_s=-20,q_y=-3],BT=-20°

e)

Offset Parabolic Cylinder Reflector Antenna

F=35GHz, PA[D=5.3m,F=1.855m,H=2.7m], AF[N=335,d=0.63λ,q_s=-20,q_y=-3],BT=37°

f)

Fig. 2. Computed Ku- and Ka-band radiation patterns in two principal planes. The green curve represents the desired beam shape and the maximum sidelobe level.

yields accurate results for both the copolarized and crosspolarized patterns with only a modest increase in computational complexity. The final performance simulations also included effects of feed offset. In the PR-2 antenna design, the Ku-band feed was placed at the focus and the Ka-band feed was offset by half the size of the Ku-

band feed. Far-field radiation patterns were then computed for various scan angles. Fig 2 shows the far field patterns in two principal planes ($\varphi=0°$, $90°$) for scan angles of $0°$, $20°$, and $37°$. Also shown, in green, is a trace that represents the desired beam shape and sidelobe envelope.

The broadside patterns at both Ku- and Ka-band show matched, symmetrical beams. The Ku-band pattern has small shoulders that violate the design template but this small deviation is deemed to be acceptable for precipitation measurements. As the beam is scanned to $20°$, the Ka-band pattern begins to show some asymmetry resulting from the asymmetrical illumination of the reflector. This changes the shape of the measurement resolution volume but the change in the overall volume is somewhat reduced since the beamwidth is shrinking in one dimension while increasing in the other. Finally, the plots at the maximum scan angle of $37°$ show some beam broadening in both planes at Ku-band and a more pronounced asymmetry at Ka-band. There is also reduction in directive gain at Ku-band. Although the resolution is somewhat degraded at the most extreme scan angles, with proper pattern calibration, useful precipitation measurements can be obtained.

4. REFLECTOR MECHANICAL DESIGN

Mechanical studies to explore design approaches and implementation feasibility, and to assess shape fidelity of the PR-2 antenna were conducted. The chosen baseline design is a cylindrical parabolic antenna featuring a metalized reflective membrane, supported by a combination of in-space rigidized inflatable tubes and rigid members. This choice was made because of its low weight, better mechanical performance, simpler deployment, better launch survivability, and low stowage volume with respect to other designs considered.

The design is driven by the aperture and antenna shape requirements; it is comprised of a reflective membrane surface described as an offset parabolic cylinder of 5.3 m in length. The parabolic profile has a linear or projected span of 5.3 m originating at the apex, and a focal length of 1.89 m.

A set of two deployable and rigidizable tubes is used to extend, tension, and maintain the desirable parabolic-cylindrical shape of the reflective membrane. The deployment is achieved by inflation of the tubes, which are subsequently rigidized to achieve greater dimensional stability and survivability from meteoroid and debris impacts. These tubes are cantilevered from the spacecraft bus and interconnected at their free-ends by a rigid cross-member.

During launch, each tube is rolled up around a rigid mandrel, and the thin-film reflective membrane is rolled up around the rigid cross-member, forming a cylindrical bundle with a launch volume no larger than a 1.3 m x 1.3 m square cross-section and 5.5 m in length. Once in space, deployment of the antenna is initiated by unfurling thecylindrical bundle from its stowed position, the deployment process is achieved through inflation of the tubes until the fully deployed antenna shape is attained (Fig. 3).

A conservative estimate of mass for this antenna design is of 75 kg. This is equivalent to an aerial density of 2.0 kg/m^2, not including the SC interface structure. The PR-2 antenna design represents a factor of 3 improvement in mass and of 7 in aperture with respect to TRMM Precipitation Radar. Current assessment indicates that, in order to meet a low sidelobe in RF signature, the antenna's
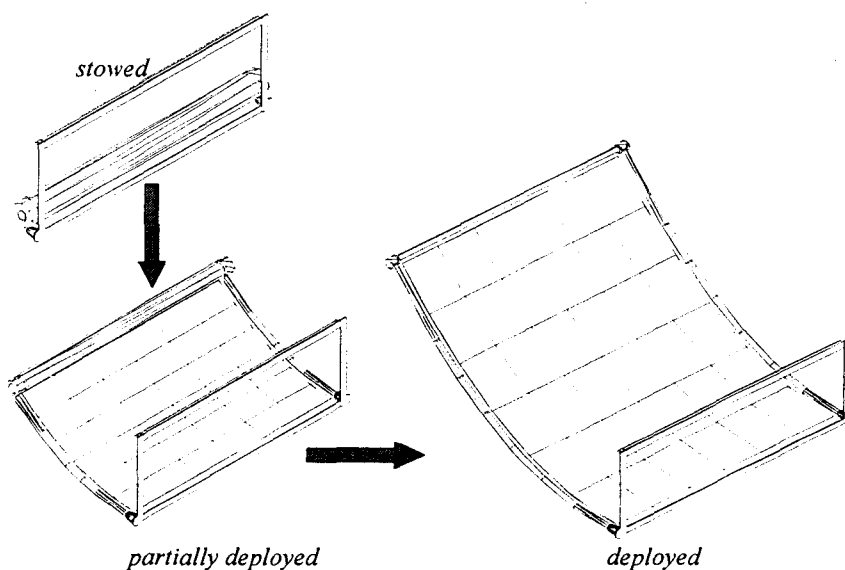

Fig. 3. Deployment Sequence

RMS surface accuracy should be better than 0.17 mm. To maintain such accuracy, the antenna design must strive for a deployed fundamental frequency of 0.5 Hz or greater, the inflatable tube must be rigidized and the reflective membrane must be dimensionally stable through the entire life of the mission.

Aperture and shape requirements are serious challenges to other designs considered, such as monolithic and segmented/deployable rigid reflective surfaces, particularly in the areas of launch viability and weight issues. In the current design, the shape fidelity and dynamic response of the reflective membrane depend not on the stiffness of the reflective surface but on the in-plane stress of the membrane, which avoids the usual challenges of stiff but brittle carbon composite reflective surfaces. Furthermore, high structural damping and low transmissivity of loads at the membrane interfaces is expected for this design.

Mechanical Analyses

Various mechanical analyses were performed, to provide a preliminary assessment of the dynamics performance and other mechanical characteristics of the design.

Table 3. Ka-band feed array requirements

Frequency	35.6 GHz
Number of elements	368
Transmitted power	1 W / module
Transmit polarization	horizontal
Receiver noise figure	4 dB
Receive polarization	horizontal, vertical
Phase Shifter bits	6
Sidelobe level	-30 dB
Crosspolarization leakage	-25 dB
Maximum scan angle	37°
Module spacing	0.65 wavelengths

A Finite Element Model (FEM) was coded and used for modal studies of the support structures and membrane, as well as in evaluations of shape distortion due to manufacturing and thermal factors.

The first one hundred modes were evaluated. Only five of those correspond to the support structure while the others are membrane modes; membrane participation is found in all of them. The first four modes of the support structure were found to be at 0.4, 1.9, 2.2, and 3.0 Hz. They correspond to various combinations of inflatable/rigidizable

a) Mode 1: first bending

b) Mode 2: Overall torsion
(anti-symmetric tube bending)

c) Mode 3: second tube bending

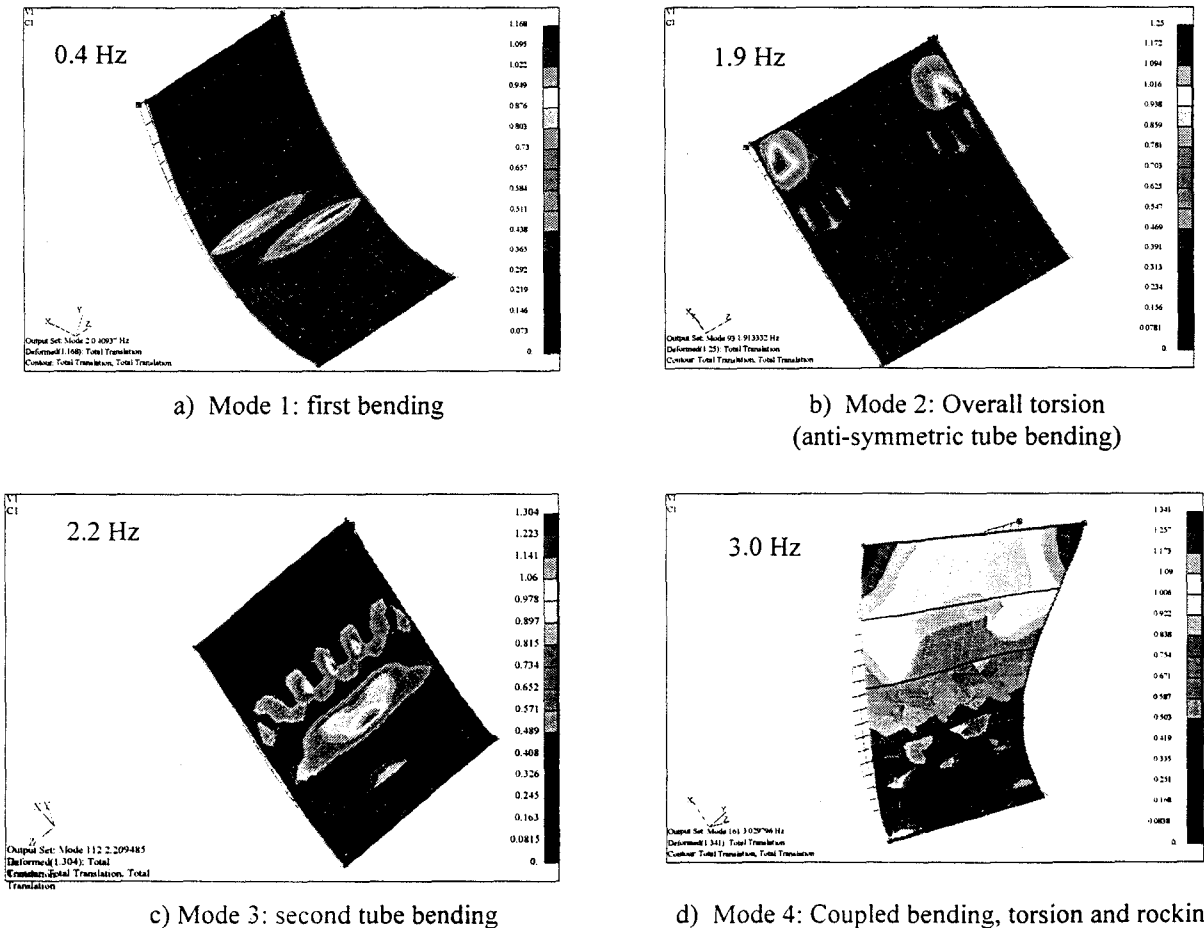d) Mode 4: Coupled bending, torsion and rocking

Fig. 4. First four mechanical modes of the membrane reflector and inflatable structure

tube simple bending. Figure 4 shows the contoured shapes for these modes. These results are from a FEM featuring 13 cm diameter inflatable/rigidizable tubes.

Membrane Shape Distortion Characterization

Studies to characterize membrane surface distortions and to assess degradation in antenna radiation patterns were conducted. The main sources for membrane shape distortion identified are permanent membrane impressions due to handling in manufacturing, manufacturing tolerances, thermal and dynamic effects.

Dynamic effects were not studied in detail, since their dependence on structural stiffness and interface details as well as spacecraft properties not currently known, would make such analyses meaningless. Dynamic effects, however, are expected to be of secondary importance due to expected high structural damping and low load transmissibility at the interfaces.

It was found that antenna overall shape distortion of greatest magnitude are those due to thermal effects, with peak values of ±2.0mm, and those due to estimated manufacturing errors, with peak values of ±1.0mm.

Future Development

Current state of the art of inflatable/rigidizable structures technologies includes a variety of methods to produce structural members, including: stretch aluminum tubes, aluminum tubes with steel ribs, UV/thermally rigidized epoxy-impregnated tubes (rigidization on command), and thermoplastic rigidization.

Irrespective of the rigidization method of choice, the antenna aperture and its mechanical requirements are sufficiently challenging to require some developments in the area of structures. Production of a scaled structural engineering model would address areas of current interest, such as verification of stiffness versus structural weight, rigidization methods and associated power requirements, geometric accuracy and fidelity, as well as structure/membrane intefaces.

In addition to development in the mechanical aspects of this type of structure, investigations and qualification of materials, both used in the inflatable/rigidizable structures and membrane constituents, for performance and survivability in space are necessary.

5. DUAL-POLARIZATION ACTIVE ARRAY FEEDS

As previously discussed, an electronically-scanned linear array feed is required to implement the adaptive cross-track scanning algorithm. The results of antenna configuration studies determined the requirements for the array feeds,

which are summarized in Table 3. Both passive and active arrays were considered. However, the high loss of precision phase shifters favors the active approach. In a passive system where phase shifter modules are fed by a single source such as a travelling wave tube amplifier (TWTA) most of the transmitter energy would be dissipated in the phase shifters and power dividers. Not only is this highly inefficient, but it would require a TWTA with output power far beyond what is currently available. In an active array, the transmitter amplifiers and receiver low-noise amplifiers are on the antenna-side of the phase shifters, effectively negating phase-shifter losses.

In order to mitigate the risk associated with development of these active arrays, an eight-element prototype of the Ka-band feed array is being developed. The Ka-band array was chosen for further development because of the much lower level of technology maturity (and higher risk) at Ka-band.

Array Size and Spacing Considerations

Complete elimination of grating lobes over the scan region of 37° from broadside requires an array spacing of 0.62 λ, where λ is the free space wavelength. However such a value of spacing would necessitate the use of a greater number of array elements (14 additional elements) and increases the difficulty of packaging module electronics. Simulations were conducted to find a spacing that is as large as possible without degrading performance unnecessarily. For a spacing of 0.64 λ, a maximum loss of about 1.4 dB at the extreme scan angles is encountered due to the presence of the grating lobe. Fig. 5 shows a plot of scan loss introduced by the onset of the grating lobe for different values of array element spacing and scan angles. The scan loss due to beam broadening effect has not been accounted for, since such an effect is common to all values of element spacing.

Design of Orthomode Transducer

An orthomode transducer (OMT) multiplexes the two linear polarization channels into the square waveguide feed. A compact OMT was designed to accommodate the 5 mm array spacing. The design of OMT was facilitated by a full wave electromagnetic analysis by the finite element method
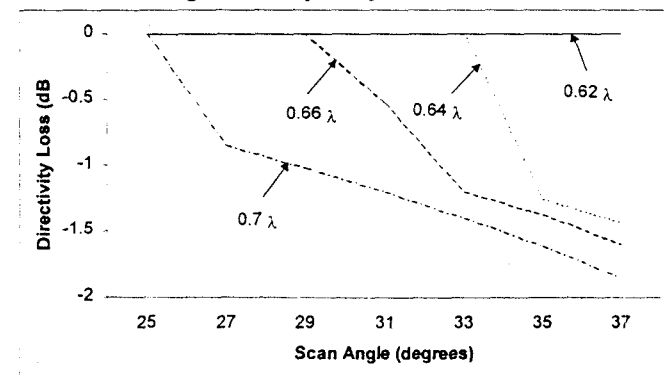
Fig. 5. Directivity loss due to grating lobes

and subsequent optimizations. By a proper choice of spacing between the inline and the orthogonal ports and matching iris (inductive and capacitive, respectively) we were able to match both ports and achieve the required polarization isolation. Subsequently we analyzed the structure for dimensional tolerance and found that a tolerance of 40 µm is adequate.

Analysis and Design of Square Waveguides Feeding Flared Corrugated Plates

Our previous study of the PR-2 antenna showed that a $\cos^{20}\theta$ radiation pattern in the vertical plane is required for the Ka-band feed array illuminating the reflector. The vertical plane pattern of a vertically polarized (E-plane) wave of the flared horn without corrugations would exhibit high sidelobes as shown in Fig. 6. It is possible to design optimum values of flare angle and the aperture size so that the two patterns coincide in the main beam region. However, without the use of corrugations it is not possible to reduce the level of these sidelobes. Since the cylindrical reflector of the PR-2 antenna is under-illuminated at Ka-band, radiation from the high sidelobes mentioned above will be scattered by the reflector and produce undesirable effects in the main beam of the reflector.

Properly designed corrugated walls reduce the sidelobes in the vertical plane for the vertically polarized wave as shown in Fig. 7. It is also noted that the patterns for both polarizations are very close to that of the $\cos^{20}\theta$ pattern
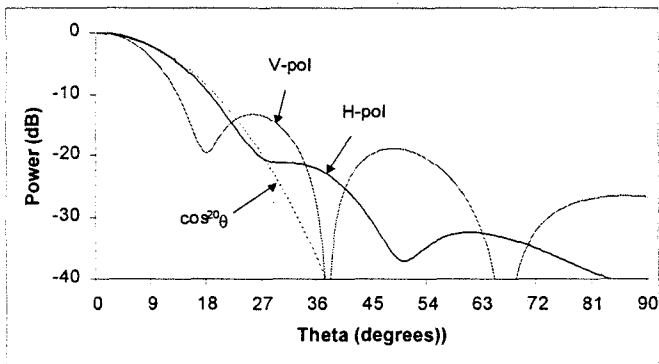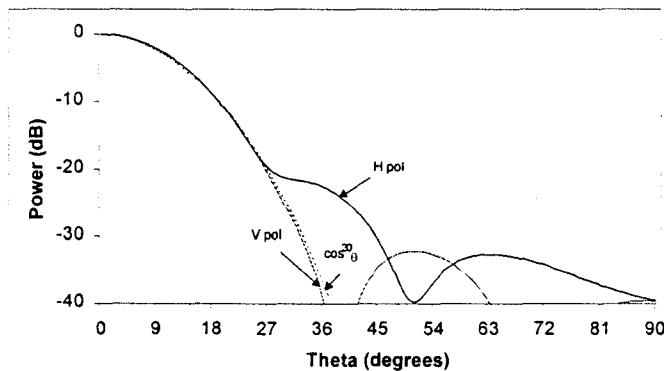

Fig. 6. Uncorrugated flared horn pattern

Fig. 7. Corrugated flared horn pattern

desired. The results in Fig. 7 were obtained by the well-known mode matching technique. Instead of using an array of flared horns, we propose to use a pair of flared corrugated walls fed by an array of square waveguides. This simplifies the manufacturing process considerably since the corrugated plates may be easily milled. Fig. 8 illustrates the structure of corrugated flared plates excited by an array of square waveguides.

In order to determine the input reflection coefficient of each waveguide port, initially we studied the problem of an infinite array of square waveguides feeding a parallel plate waveguide system. This problem is easier to model analytically by a full wave electromagnetic code. Again, the finite element analysis yielded the value of reflection coefficient as a function of scan angle, as illustrated in Fig. 9. Note that the reflection coefficient is generally small for the vertical polarization (TE_{10} mode excitation) and for smaller values of scan angles in the case of horizontal polarization (TE_{01} mode excitation). Our studies on wide-angle impedance matching with a single dielectric sheet did not produce significant improvements to the input reflection coefficients for both polarizations. Note that over a wide range of scan angles the reflection coefficient is either small or constant. Therefore a tuning arrangement at the input port of each polarization separately would be adequate for matching, except for large values of scan angles for the
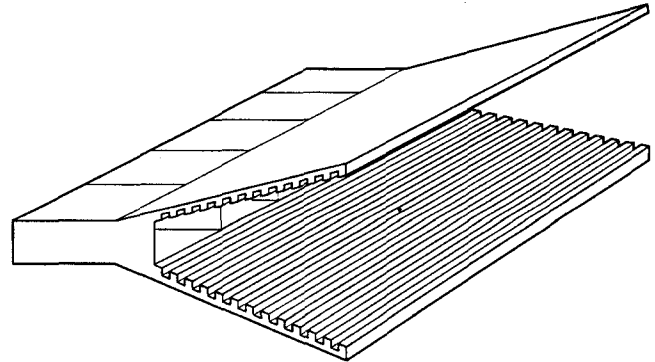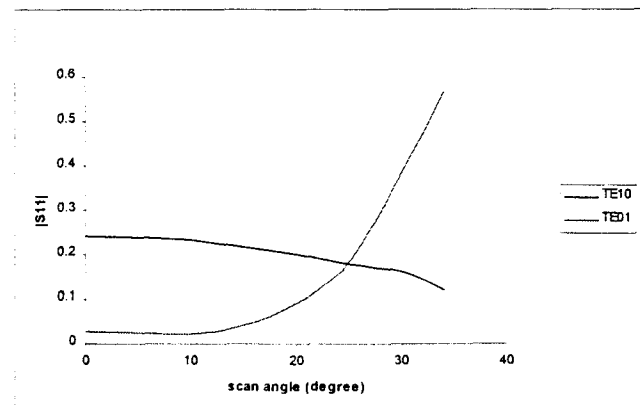

Fig 8. Corrugated, flared horn configuration

Fig. 9. Element reflection coefficients

horizontal polarization. Since the PR-2 radar uses the horizontal polarization only for reception, we may tolerate a higher value of mismatch, especially for large values of scan angles.

We also studied the reflection coefficient at an input port of an infinite array of square waveguides with flared corrugated plates. These results were found to be similar to those in Fig. 6. This shows that the reflection occurs primarily at the junction of the square waveguides and the flared plates. In the experimental model of a small finite array we plan to use some dummy elements at each end. We are planning to study the reflection coefficient of a finite array using the method of moments solutions to the pertinent coupled integral equations.

T/R module design

The overall system requirements and the results of antenna configuration studies determined the requirements for the T/R modules, which were summarized in Table 3. A preliminary design for this module has been created and development of a prototype is currently underway.

The baseline block diagram for the Ka-band T/R module is show in Fig. 10. It is composed of a transmitter channel and two identical receiver channels. One of the receive channels is duplexed with the transmitter channel using MMIC switches. Each channel contains a mixer for up or down conversion, an image filter, a phase-shifter and a suitable amount of amplification. Use of up and down conversion within the module while increasing complexity has two main advantages; it allows lower frequency phase shifters to be used and it reduces losses in the divider/combiner networks, permitting the use of simple stripline and microstrip dividers rather than complex, bulky and expensive waveguide manifolds.

The 368-element array is divided into 46 subarrays of 8 elements each. Each subarray contains signal divider/combiner networks for both polarization channels and for the local oscillator (LO). These will be implemented as 8-way corporate dividers in a multilayer microwave substrate. The center layer will contain the LO divider, implemented in stripline while the top and bottom surface will contain the V and H channel dividers, which will be implemented in microstrip.

Each subarray will share a common control and bias module (CBM). The CBM will receive DC power from the spacecraft bus and will generate all operating voltages required by the T/R modules. The CBM will also receive commands from the array controller and will command the phase shifters and switches within each module. By sharing the bias generation and control functions between eight modules, the complexity of the module electronics is drastically reduced.

The circuitry within each module has been designed to employ currently available MMICs and relatively mature technologies. The X-band IF within the module permits the use of a wide range of components available for that frequency range, including high-precision phase shifters. Subharmonically pumped mixers are used for both up and down conversion, thereby eliminating the need to generate and distribute a 25 GHz LO signal.

The major design challenge in implementing the T/R modules is thermal management and compensation. Each module will generate 1 W output power with a duty cycle of up to 25%. Due to the efficiency of the power amplifiers and other amplifier monolithic microwave integrated circuits (MMICs) the overall power dissipation for each module will be several watts. The bias voltages and circuitry will be optimized to minimize power consumption while yielding adequate performance.

In addition to the problem of managing waste heat, there is the problem of thermal compensation. Due to changing solar illumination the array can experience large temperature swings over an orbit. The gain of amplifier MMICs in both the receiver and transmitter channels is strongly affected by temperature. In order to insure that the transmitter power and the receiver gain are sufficiently stabilized, some form of compensation is required. Our initial approach to this problem includes both active and passive gain compensation methods.

The passive approach uses Thermopads™, which are constant impedance attenuators that change insertion loss with temperature. These devices are simple, rugged and require no DC power. However, to achieve the required compensation range, large values of attenuation are required. This requires inclusion of additional amplifier stages which increases module complexity and power consumption. Automatic gain control (AGC) amplifiers can be used to supplement the passive compensation. A temperature sensing circuit controls the gain of these amplifiers, according the measured temperature/gain characteristics of the whole signal chain. This circuit can be tailored to remove the mismatch between the temperature coefficient of the Thermopad™ and signal chain gain drift characteristics.

6. REAL-TIME DIGITAL PULSE COMPRESSION

To achieve the required resolution and sensitivity without using impractical peak power levels, a linear frequency modulated (LFM) chirp waveform is used. LFM chirps have been used successfully for decades in various radar systems but their use in down-looking atmospheric radar presents special challenges.
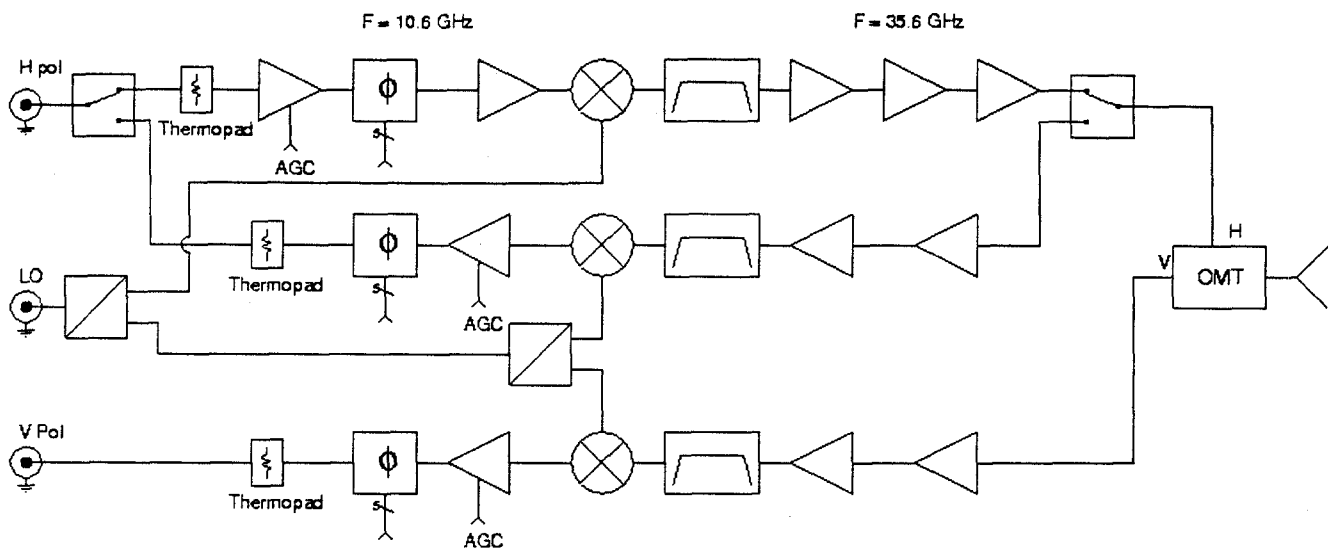
F = 10.6 GHz   F = 35.6 GHz

Fig. 10. Block diagram of T/R module baseline design

In chirped radar systems, a long LFM pulse (up to 40 µs, in this case) is transmitted. The echo signal is then correlated with the original pulse waveform, yielding temporal resolution approximately equal to the reciprocal of the pulse bandwidth. However, in addition to the main correlation peak, spurious correlations occur. These are referred to as time or range sidelobes and are analogous to antenna sidelobes. These sidelobes are particularly troublesome for a precipitation radar pointing at nadir because the surface echo power can be as much as 60 dB larger than echoes from precipitation very close to the surface. Thus, the range sidelobes need to be suppressed 60 dB with respect to main correlation peak.

The two main approaches to correlation are digital pulse compression and analog pulse compression using dispersive filters such as surface acoustic wave (SAW) devices. SAW filters operate in real time but typically yield sidelobe levels no better than -35 dB. Digital pulse compression techniques permit compensation for non-ideal characteristics of the system (provided that they are well characterized) and can provide substantially better sidelobe suppression. Experiments with JPL's Airborne Rain Mapping Radar (ARMAR) demonstrated sidelobe suppression of up to 60 dB [3]. However, this was achieved by recording all radar echoes on a high-speed tape recorder and processing them later. While this technique has been used for spaceborne synthetic aperture radars (SARs), SAR systems only collect data intermittently, while a precipitation radar collects data continuously. Since continuous operation is required, and it is not practical to downlink large volumes of raw echo data, a real time processing solution is required.

The first step in the development of the real-time digital pulse compression system is the development of an airborne breadboard system. Such a system is being developed using a combination of custom and commercial-off-the-shelf

(COTS) VME hardware. The system has three main components, a two channel (one for Ku-band, one of Ka-band) arbitrary waveform generator (AWG), a four channel (two received polarizations by two frequencies) acquisition board and a programmable digital signal processor board which uses Xilinx field programmable gate arrays (FPGAs).

The PR-2 airborne breadboard uses a custom 12 bit analog-to-digital converter (ADC) board based on an Analog Devices 14 bit converter, which provides four simultaneously sampled and processed channels (Ku and Ka, H and V receive channels). Data is oversampled a factor of 2 above Nyquist limit (20 MHz) and then digitally low-pass filtered and decimated by a factor of two. Using a digital filter as the main video filter allows more precise control of the filter characteristics and eases the requirements on the analog antialiasing filter.

The transmit waveform is generated by a custom two channel AWG which yields 14 bits resolution at a sample rate of 40 Msamples/s. Using AWGs instead of a traditional numerically controlled oscillator has two major advantages. The AWG can be used to implement amplitude weighting of the pulse that substantially reduces range sidelobes at the expense of slightly degrading range resolution. Secondly, the AWG allows a predistortion to be applied to the transmit waveform in order to partially compensate for nonideal characteristic of the system. While, in a perfectly linear system, it is mathematically equivalent to compensate for these effects in the receive processing, dividing the distortion compensation between transmit side and receive side reduces quantization noise. Also, by producing a chirp that is spectrally flat at the transmitter output, it is easier to see small changes during test and calibration. The compensation calibration technique uses a closed loop algorithm which incrementally changes the transmit pulse to get the desired results at its feedback point.

The real-time signal processor card is a COTS VME card made by Annapolis Microsystems. The board contains three large Xilinx Vertex FPGAs; reprogrammable parts which can be configured as almost any kind of digital logic. With four channels, the system performs 20 billion multiplications and 20 billion additions per second. This processing throughput would be difficult to achieve with microprocessors. FPGAs enable implementation of efficient algorithm specific circuitry without the nonrecurring costs and development time associated with application specific integrated circuits (ASICs). The highly parallel implementations possible with FPGAs allow realization of the entire real-time processor in only two chips.

The front-end of the processor is four 64-tap, 16-bit finite impulse response (FIR) filters implemented with bit serial multipliers clocking at 133 MHz. The filter receives 20 MHz offset video, and selects 4 MHz flat bandwidth centered around 5 MHz, with 70 dB suppression of the 4-MHz band centered around DC. Following the filter is a downsampling and digital IQ demodulation yielding in-phase and quadrature baseband signals. The output data is complex and clocked at 5 MHz.

Following the video filter is a matched filter stage. This is a 256 tap complex FIR filter (actually 4 real integer FIR filters) loaded with a 12 bit reference function clocking at 5 MHz. The reference function we use is a Kaiser window (K=6) squared envelope modulated on an ideal chirp which has be modified slightly to tune out system distortion.

For every range sample, the copolarized and crosspolarized echo power is computed. The pulse pair technique is used to calculate the mean Doppler velocity and the Doppler spectral width. The power and pulse-pair estimates from 64 pulses are then averaged, yielding a 64-fold reduction the output data rate. Any echo containing a saturated ADC value is dropped from the averages because even a single clipped ADC sample creates large sidelobes which can obscure much of the useful data near the ocean surface. The averaging and resulting reduction in data rate is possible only after pulse compression and calculation of power and pulse-pair estimates has been performed.

An FPGA processor implementation has been developed and is currently undergoing laboratory testing. Fig. 11 shows the time domain response of 64 averaged pulses. This resulted from generating sampled data from 64 pulse waveforms, adding white noise placing this data into the processors input buffers. The FPGA processor then performed all of the steps previously described to generate the output shown in Fig. 11. This plot demonstrates sidelobe suppression of greater than 70 dB. This test validates the algorithm and FPGA program but does not include the non-ideal characteristics of the transmitter. Full system performance, with compensation will be demonstrated after
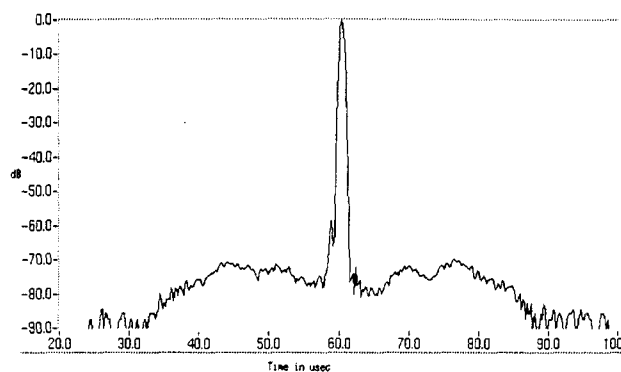

Fig. 11. Time domain pulse compressor output

the digital signal processor is integrated into the full PR-2 breadboard system.

7. CONCLUSIONS

Following the success of the TRMM PR concepts for the second generation of spaceborne precipitation radars were investigated. A system concept using a large deployable membrane antenna, an electronically scanned dual-frequency, dual polarization feed array and real-time digital pulse compression has been developed. In order to support realization of this instrument design, several parallel technology development tasks have been initiated.

Both the electrical and mechanical design of the reflector have been carefully studied. Study results indicate that this antenna would yield acceptable performance and can be implemented using current membrane and inflatable rigidizable structure technology. The next step is to build a breadboard model of this reflector and demonstrate its mechanical stability.

A design for a scanning feed system has also been created and analyzed and development of the Ka-band subarray prototype is underway. Production of a Ka-band T/R module with integrated miniature OMT will take place next year with integration and testing of an 8-element subarray to follow.

We have also developed a real-time digital signal processing system that will be integrated into the PR-2 airborne breadboard. This system will be used to capture real precipitation data from an airborne platform and will provide an opportunity to test and refine the real-time signal processing algorithms. In a separate, parallel effort a custom FPGA processor board is being developed. This board will be a space flight compatible design and will incorporate additional circuitry to mitigate the effects of radiation induced single-event upsets.

By aggressively developing these underlying technologies, much of the risk associated with implementation the Second Generation Spaceborne Precipitation Radar can be retired

prior to the start of the flight instrument development. This will allow future precipitation radar missions to incorporate more capable instruments and will benefit the science community by vastly increasing satellite coverage as well as increasing the accuracy of retrieved rain rates.

REFERENCES

[1] Okamoto, K., T. Iguchi, T. Kozu, H. Kumagai, J. Awaka, and R. Meneghini, 1998: Early results from the Precipitation Radar on the Tropical Rainfall Measuring Mission. CLIMPARA'98, 8 pp.

[2] Im, Eastwood, S. Durden, G. Sadowy, A. Berkun. J. Huang, M. Lou, B. Lopez, Y. Rahmat-Samii, S. Rengarajan, 2000: System Concept for Next Generation Spaceborne Precipitation Radars. *Proceedings of the IEEE Aerospace Conference,* Big Sky, Montana, USA

[3] A. Tanner, S. L. Durden, R. Denning, E. Im, F. K. Li, W. Ricketts, W. Wilson, "Pulse compression with very low sidelobes in an airborne rain mapping radar," *IEEE Trans. Geosci. Remote Sensing,* 32, 211-213, 1994.

Gregory Sadowy received his Ph.D. degree in electrical engineering from the University of Massachusetts. He has extensive experience in the development of meteorological radar systems. He designed and managed development of the RF electronics for the NASA/JPL 95-GHz Airborne Cloud Radar and is currently supporting the RF electronics development for both the 94-GHz spaceborne cloud radar and the Second-Generation Precipitation Radar breadboard. Dr. Sadowy is also involved in the design of advanced radar architectures using microwave photonics technology.

Andrew Berkun is a Digital Engineer at JPL. He has been actively involved in the digital electronics design, implementation, and testing in many spaceborne and airborne radar programs at JPL, including the Cassini Radar for remote sensing of Titan, Shuttle Imaging Radar-C, JPL

Stephen L. Durden is a Senior Engineer at JPL and has contributed to the development of Airborne Rain Mapping Radar and Airborne Cloud Radar, and to the design of spaceborne synthetic aperture radar (LightSAR). He is currently a member of the TRMM Postlaunch Validation Team, and the System Engineer for both the Second-Generation Precipitation Radar breadboard, and the 94-GHz cloud profiling radar for the ESSP CloudSat Mission. He has also been actively engaged in microwave remote sensing research, including modeling of microwave scattering and data analysis. He is author or co-author of over 35 journal publications.
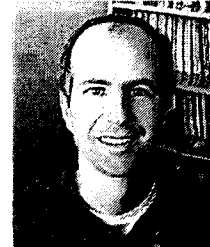
John Huang received his Ph.D. degree in electrical engineering from the Ohio State University. He worked six years at the Naval Weapons Center, China Lake, CA, where his principle duties were design and development of conformal antennas and RCS analysis by GTD. He has been with JPL since 1980, where his research activities involve microstrip antennas, mobile vehicle antennas, spacecraft antennas, phased arrays, and inflatable antennas. Dr. Huang, an IEEE Fellow, has published more than eighty journal and conference papers, three book chapters, and received three U.S. patents and more than fifteen NASA Certificates of Recognition. He is currently appointed as IEEE Distinguished Lecturer and has also been an invited speaker in various international symposia and short courses

Eastwood Im is the Radar Instrument Manager of the NASA ESSP CloudSat Mission. He is also the Supervisor of the Atmospheric Radar Science and Engineering Group at JPL. He has extensive experience in spaceborne meteorological radar science and remote sensing, and advanced radar system studies. Dr. Im is the Principal Investigator of TRMM radar calibration study and a member of the TRMM Science Team, and the Principal Investigator of the NASA IIP Second-Generation Precipitation Radar (PR-2) task. He has been a member of Science Steering Group for the EOS-9 Global Precipitation Mission since the start of the planning phase. Dr. Im is the Associate Editor of the AMS Journal of Atmospheric and

Oceanic Technology. He has over 80 refereed journal and conference publications.

Michael C. Lou has worked on the development of structural systems and structures technologies for over 28 years. He received his doctorate degree in aerospace engineering from the University of Michigan at Ann Arbor in 1973 where his thesis was on non-linear dynamics. Dr. Lou joined JPL in 1980 after working at Ford Motor Company for 7 years. At JPL, Dr. Lou has held a variety of technical and managerial positions, including task manager, group leader, group supervisor, deputy section manger, and lead technologist. He is currently leading several gossamer space structures technology development efforts and is the Co-PI of the Inflatable Sunshield In Space (ISIS) space experiment. ISIS is scheduled to be flown in the Shuttle in early 2001 to validate space inflatables technology for possible application to the Next Generation Space Telescope. Dr. Lou has also been assigned JPL's Technology Community Leader for Large Ultra-lightweight Space structures.

Bernardo C. Lopez received his B.S. degree in Aerospace Engineering from California State Polytechnic University in Pomona in 1991 and is currently finishing his Masters Degree in Mechanical Engineering from California State University, Los Angeles. From 1991 to 1998, he was with TRW Space and Electronics as an analyst in the Structural Dynamics Department, performing structural analyses and tests on satellite structures, as well as conducting studies on deployment of mechanisms. Mr. Lopez joined JPL in June of 1998 and has been working on the development of inflatable structures technologies and their insertion to future space missions.

Yahya Rahmat-Samii (S'73-M'75-SM'79-F'85) is a Professor of Electrical Engineering at the University of California, Los Angeles (UCLA). He was a Senior Research Scientist at NASA's Jet Propulsion Laboratory/California Institute of Technology before joining UCLA. He was a Guest Professor at the Technical University of Denmark (TUD) in the summer of 1986. He has also been a consultant to many aerospace companies. He received the M.S. and Ph.D. degrees in Electrical Engineering from the University of Illinois, Urbana-Champaign.

Dr. Rahmat-Samii was the 1995 President and 1994 Vice-President of IEEE Antennas and Propagation Society. He was appointed an IEEE Antennas and Propagation Society Distinguished Lecturer and presented lectures internationally. Dr. Rahmat-Samii was elected as a Fellow of IEEE in 1985 and a Fellow of IAE in 1986. He was also a member of the Strategic Planning and Review Committee (SPARC) of IEEE. He has been the guest and plenary session speaker at many national and international symposia. He was one of the directors and Vice President of the Antennas Measurement Techniques Association (AMTA) for three years. He has been editor and guest editor of many technical journals and book publication entities. He has also served as Chairman and Co-Chairman of several national and international symposia. Dr. Rahmat-Samii was also a member of UCLA's Graduate council for a period of three years.

Dr. Rahmat-Samii has authored and co-authored over 450 technical journal articles and conference papers and has written fourteen book chapters. He is the co-author of two books entitled, *Electromagnetic Optimization by Genetic Algorithms, and Impedance Boundary Conditions in Electromagnetics* published in 1999 and 1995, respectively. He is also the holder of several patents. He has had pioneering research contributions in diverse areas of electromagnetics, antennas, measurement and diagnostics techniques, numerical and asymptotic methods, satellite and personal communications and human/antenna interactions, etc. (visit http://www.antlab.ee.ucla.edu). For his contributions, Dr. Rahmat-Samii has received numerous NASA and JPL Certificates of Recognition. In 1984 he was the recipient of the prestigious Henry Booker Award of URSI. In 1992 and 1995, he was the recipient of the Best Application Paper Award (Wheeler Award) for papers published in the 1991 and 1993 IEEE AP-S Transactions. In 1993, 94 and 95, three of his Ph.D. students were named the Most Outstanding Ph.D. Students at UCLA's School of Engineering and Applied Science. Five others received various Student Paper Awards at the 1993, 1996, 1997 and 1998 IEEE AP-S/URSI Symposiums. He has recently been selected as one of the recipients of the IEEE Millennium Medals. Dr. Rahmat-Samii is a member of Commissions A, B and J of USNC/URSI, AMTA, Sigma Xi, Eta Kappa Nu and the Electromagnetics Academy. He is listed in Who's Who in America, Who's Who in Frontiers of Science and Technology and Who's Who in Engineering. In 1999, he was the recipient of Distinguished Alumni Award of the University of Illinois, ECE. In 2000, he was the recipient of the IEEE Third Millennium Medal and the AMTA Distinguished Achievement Award.

Sembiam Rengajaran is the Professor in Electrical Engineering at California State University at Northridge. His research interests include analytical and numerical techniques in electromagnetics with applications to antennas, scattering, and passive microwave components. He has authored/co-authored 145 journal and conference papers. He is a Fellow of the IEEE, a member of USNC/URSI Commission B, and the Electromagnetics Academy. He served as the chair of the LA Chapter of IEEE Antennas and Propagation Society (1983-84) and the San Fernando Valley Section of IEEE (1995). Dr. Rengajaran has served as a consultant to many government agencies and private industry.